Bioorganic & Medicinal Chemistry Letters xxx (2018) xxx–xxx

Contents lists available at ScienceDirect

Bioorganic & Medicinal Chemistry Letters

journal homepage: www.elsevier.com/locate/bmcl

Design, synthesis, SAR and biological investigation of 3-(carboxymethyl) rhodanine and aminothiazole inhibitors of *Mycobacterium tuberculosis* Zmp1

Mattia Mori [a,b], Davide Deodato [a], Mohan Kasula [a], Davide M. Ferraris [c], Adriana Sanna [d], Alessandro De Logu [e], Menico Rizzi [c], Maurizio Botta [a,f,*]

[a] Department of Biotechnology, Chemistry and Pharmacy, University of Siena, via Aldo Moro 2, 53019 Siena, Italy
[b] Center for Life Nano Science@Sapienza, Istituto Italiano di Tecnologia, viale Regina Elena 291, 00161 Roma, Italy
[c] DiSF-Dipartimento di Scienze del Farmaco, Università del Piemonte Orientale, Via Bovio 6, 28100 Novara, Italy
[d] Department of Public Health, Clinical and Molecular Medicine, University of Cagliari, Via Porcell 4, 09124 Cagliari, Italy
[e] Department of Life and Enviromental Sciences, University of Cagliari, Via Porcell 4, 09124 Cagliari, Italy
[f] Sbarro Institute for Cancer Research and Molecular Medicine, Center for Biotechnology, College of Science and Technology, Temple University, BioLife Science Bldg., Suite 333, 1900 N 12th Street, Philadelphia, PA 19122, USA

ARTICLE INFO

Article history:
Received 30 November 2017
Revised 16 January 2018
Accepted 17 January 2018
Available online xxxx

Keywords:
Rhodanines
Aminothiazoles
Zmp1
Tuberculosis
Metalloproteases

ABSTRACT

Sixteen 3-(carboxymethyl)rhodanines, and twelve aminothiazoles as rhodanine-mimetics were designed, synthesized and tested as inhibitors of the Zmp1 enzyme from *Mycobacterium tuberculosis* (Mtb). Almost all rhodanines (**5a–d**, **5f–n**, and **7a–b**) exhibited Zmp1 inhibition with IC_{50} values in the range 1.3–43.9 μM, whereas only aminothiazoles **12b** and **12d** proved active with IC_{50} values of 41.3 and 35.7 μM, respectively. Structure-activity relationships (SAR) were coupled with molecular modeling studies to highlight structural determinants for Zmp1 inhibition. Moreover, rhodanines **5a** and **5c** induced 23.4 and 53.8% of Mtb growth inhibition in THP-1 infected cells, respectively, at the non-toxic concentration of 10 μg/ml. This work represents a step forward in targeting Zmp1 by small molecules.

Tuberculosis (TB) is an infectious disease caused by *Mycobacterium tuberculosis* (Mtb) that has been one of the top ten causes of death worldwide in 2015.[1] To control TB spread, in the '90s the WHO has launched the DOTS (Directly Observed Treatment, Short Course) strategy that proved successful in effectively achieving cure rates over 90% in countries where the health system works well. On the contrary, DOTS proved notably less successful in cases of HIV co-infections or in patients infected by multidrug-resistant (MDR), extensively drug-resistant (XDR) and totally drug-resistant (TDR) Mtb strains.[2–4] Therefore, novel and effective strategies to treat and control TB are still urgently needed, and may be achieved by targeting Mtb validated targets or Mtb proteins that are relevant for its replication and survival into the host.[5–7] In this context, Mtb-secreted extracellular proteins are attracting much interest either as candidate drug targets or biomarkers of active and latent TB, mostly because of their predominant role in virulence, in mediating host-pathogen interaction, and in attenuating host immune response.[8–10] Among them, the extracellular zinc metalloprotease 1 (Zmp1)[11–13] has been reported to play a key role in phagosome maturation and to elicit TB-specific humoral immune response,[14] thus enhancing the overall survival of Mtb in the host. In a guinea pig model of TB infection, Zmp1 deletion has led to increase the protective efficacy of the live vaccine *Mycobacterium bovis* BCG,[12] in agreement with Master et al.,[15] showing that Zmp1 deletion is associated to virulence attenuation. In contrast, Muttucumaru et al. have showed that deletion of the Zmp1 gene leads to bacterial hypervirulence in a murine model.[16] Nevertheless, it is clear from multiple reports that Zmp1 plays a relevant role in host–pathogen interaction, and that the design of specific small molecule inhibitors could be a valuable strategy towards anti-TB therapeutics. Zmp1 inhibitors may also serve as tools to further understanding the pathogenic role of Zmp1.

Based on the available X-ray structure of Zmp1/ligand complex,[17] we recently identified the 3-(carboxymethyl)rhodanine as privileged scaffold of Zmp1 inhibitors by disclosing **ZTB23(R)**, **ZTB28(R)** and **ZTB29(R)** (Fig. 1) as confirmed hits.[18] Subsequent

* Corresponding author at: Department of Biotechnology, Chemistry and Pharmacy, University of Siena, via Aldo Moro 2, 53100 Siena, Italy.
E-mail address: botta@unisi.it (M. Botta).

https://doi.org/10.1016/j.bmcl.2018.01.031
0960-894X/

to our work, two reports on rhodanine and quinolidene-rhodanine Zmp1 inhibitors have been published.[19,20]

Here, to further understanding the structure–activity relationships (SAR) of the 3-(carboxymethyl)rhodanine scaffold and to investigate its effect on Mtb growth, we designed, synthesized and tested *in silico* and *in vitro* sixteen rhodanines and twelve aminothiazoles as possible rhodanine-mimetics (Fig. 1).

Particularly, we modified *i*) the amino acid moiety of rhodanines responsible for zinc coordination,[18] *ii*) the nature of the aromatic ring linked to the rhodanine core, and *iii*) the position and type of substituents to the phenyl ring (Fig. 1). Moreover, to understand the relevance of the rhodanine core, it was replaced by the aminothiazole moiety (Fig. 1). The preparation of the rhodanine derivatives followed the synthetic route already described previously (see also Supporting Information for chemistry directions and compounds characterization).[18] Briefly, D-amino acids **1a**–**c** were reacted with carbon disulfide in water to give compounds **2a**–**c**, which were treated *in situ* with sodium chloroacetate and lastly with HCl, affording cyclized compounds **3a**–**c**. Knoevenagel condensation with the opportune benzaldehydes **4a**–**i**, using β-alanine as base (Scheme 1), furnished the final Z-rhodanines **5a**–**n** listed in Table 1. ^{1}H NMR analysis of compounds **5a**–**n** confirmed the presence of a single peak for the olefin proton (CH=) in the range of 7.70–7.50 ppm, at lower field values than expected for the *E*-isomer. This observation suggests the *Z* configuration of the double bond due to the higher termodynamic stability of this isomer.[21,22] Heteroaromatic derivatives **7a**–**b** bearing a pyridine and a thiophene substituent were similarly obtained by using the corresponding heteroaromatic aldehydes **6a**–**b** (Scheme 2).

Aminothiazole derivatives were obtained as outlined in Scheme 3. Starting material was D-phenylalanine **1a**, which was converted to the corresponding methyl ester **8** by treatment with thionyl chloride in methanol. Compound **8** was then reacted with methoxycarbonyl isothiocyanate, using DIPEA as the base, to give the *N*-methoxycarbonylthiourea **9** that was hydrolyzed with sodium hydroxide to furnish the thiourea **10**, bearing a free carboxylic acid function. The aminothiazole products were synthesized according to the Hantzch thiazole synthesis,[23] in which

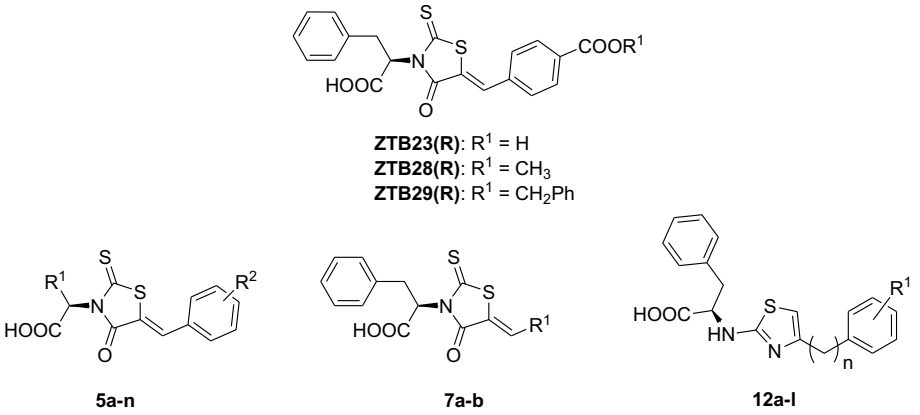

Fig. 1. Chemical structure of Zmp1 inhibitors **ZTB23(R)**, **ZTB28(R)** and **ZTB29(R)** identified previously (top),[18] and rational design of novel rhodanine and aminothiazole derivatives investigated in this work as Zmp1 inhibitors (bottom).

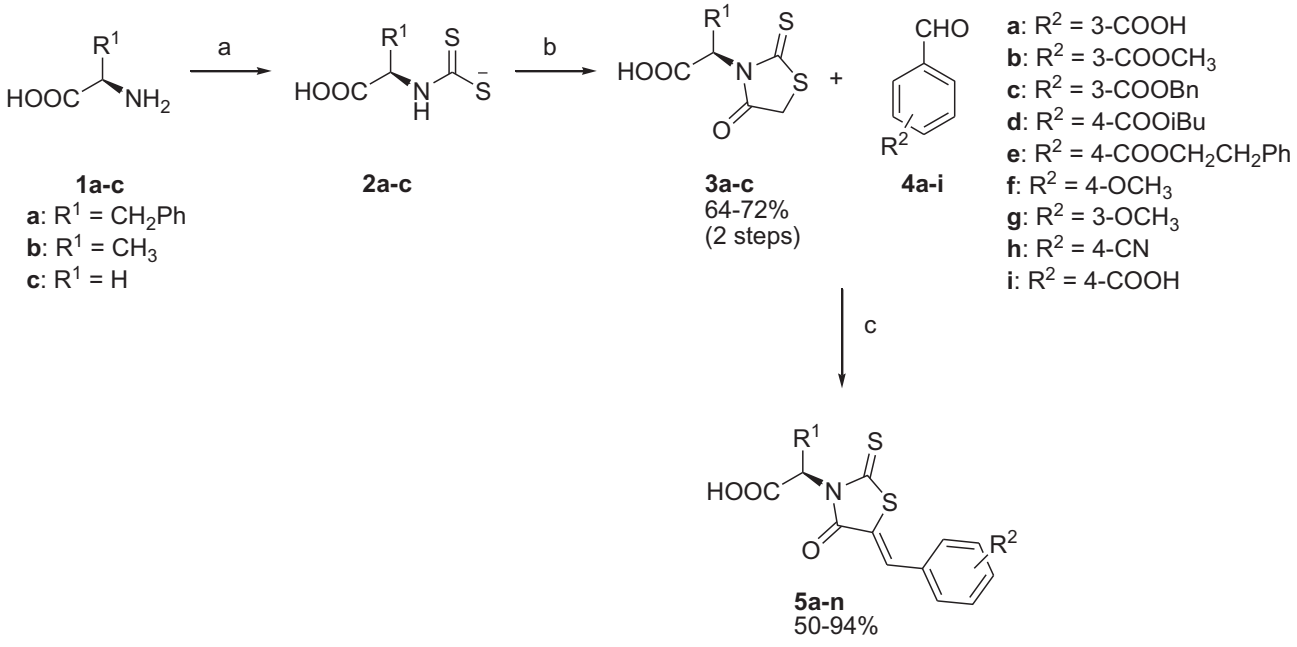

Scheme 1. [a]*Reagents and conditions*: (a) carbon disulfide, NaOH, H_2O, r.t. 12 h; (b) *i.* sodium chloroacetate solution, r.t. 2 h; *ii.* 6 N HCl, cat. $POCl_3$, 75 °C, 4 h; (c) β-alanine, AcOH, ref, 6 h.

Please cite this article in press as: Mori M., et al. Bioorg. Med. Chem. Lett. (2018), https://doi.org/10.1016/j.bmcl.2018.01.031

Table 1
Substitution patterns of final compounds **5a–n**.

Cmpd	R^1	R^2	Cmpd	R^1	R^2
5a	Ph	3-COOH	**5h**	Ph	4-CN
5b	Ph	3-$COOCH_3$	**5i**	CH_3	4-COOH
5c	Ph	3-COOBn	**5j**	CH_3	3-COOH
5d	Ph	4-COOiBu	**5k**	CH_3	3-OCH_3
5e	Ph	4-$COOCH_2CH_2Ph$	**5l**	H	4-COOH
5f	Ph	4-OCH_3	**5m**	H	3-COOH
5g	Ph	3-OCH_3	**5n**	H	3-OCH_3

Table 2
Substitution patterns of final compounds **12a–l**.

Cmpd	n	R	Cmpd	n	R
12a	0	3-OCH_3	**12g**	1	H
12b	0	4-CN	**12h**	1	3-OCH_3
12c	0	4-OCH_3	**12i**	1	4-$COOCH_3$
12d	0	4-NO_2	**12j**	1	3-$COOCH_3$
12e	0	4-COOH	**12k**	1	4-COOH
12f	0	3-COOH	**12l**	1	3-COOH

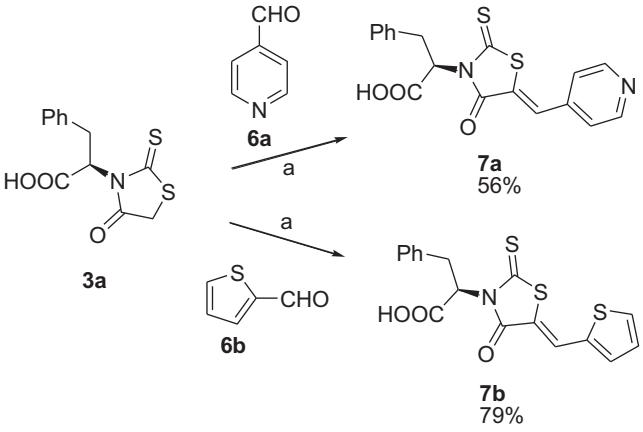

Scheme 2. [a]*Reagents and conditions*: (a) β-alanine, AcOH, ref, 6 h.

thiourea **10** was condensed with the opportune α-bromo acetophenone **11a–j** in dimethylformamide. The desired products **12a–j** were obtained after a single purification step in good overall yields (40–78%). Dicarboxylic derivatives **12k–l** were obtained after saponification of the corresponding methyl esters **12i–j**.

Commercially unavailable α-bromoacetophenones **11g–j** were synthesized starting from the corresponding phenylacetic acids **14g–j**. The methylene group was inserted with a two-step protocol of chlorination and reaction with (trimethylsilyl)diazomethane, furnishing intermediates **15g–j**. *In situ* cleavage of the trimethylsilyl groups with hydrobromic acid in anhydrous acetonitrile, afforded the desired α-bromoacetophenones **11g–j**. Unavailable carboxymethyl-phenylacetic acids **14i–j** were prepared by palladium-catalyzed arylation of acetic acid, using the appropriate aryl iodide **13i–j** as starting material (Scheme 4).

Zmp1 inhibitory activity of synthesized compounds was first evaluated at a fixed dose of 50 μM (Table 3). IC_{50} was then calculated only for molecules showing less than 40% of Zmp1 residual activity, as well as for the reference Zmp1 inhibitor **ZTB23(R)** that was included for comparison (experimental data in Supporting Information). Results are reported in Table 3, and clearly show that rhodanine derivatives are potent inhibitor of Zmp1, whereas aminothiazoles showed only a modest inhibition.

The following SAR can be drawn from data of Table 3. In rhodanines bearing D-phenylalanine as Zn-binding group (**5a–h** and **7a–b**), the introduction of small and lipophilic substituents to the distal phenyl ring in *meta* or in *para* position does not affect significantly Zmp1 inhibition (**5f** and **5g** share a similar potency), whereas the introduction of a carboxylic function in *meta* (compare **5a** and **ZTB23(R)**) or the esterification of a carboxylic acid in any positions is detrimental for activity (compare **5b–c** with **5a**, and **5d–e** with **ZTB23(R)**). In contrast, bulky esters are allowed only in *meta* to the distal phenyl ring (compare **5c** with **5d–e**). A nitrile group in *para* position is well tolerated (**5h**) and leads to the stron-

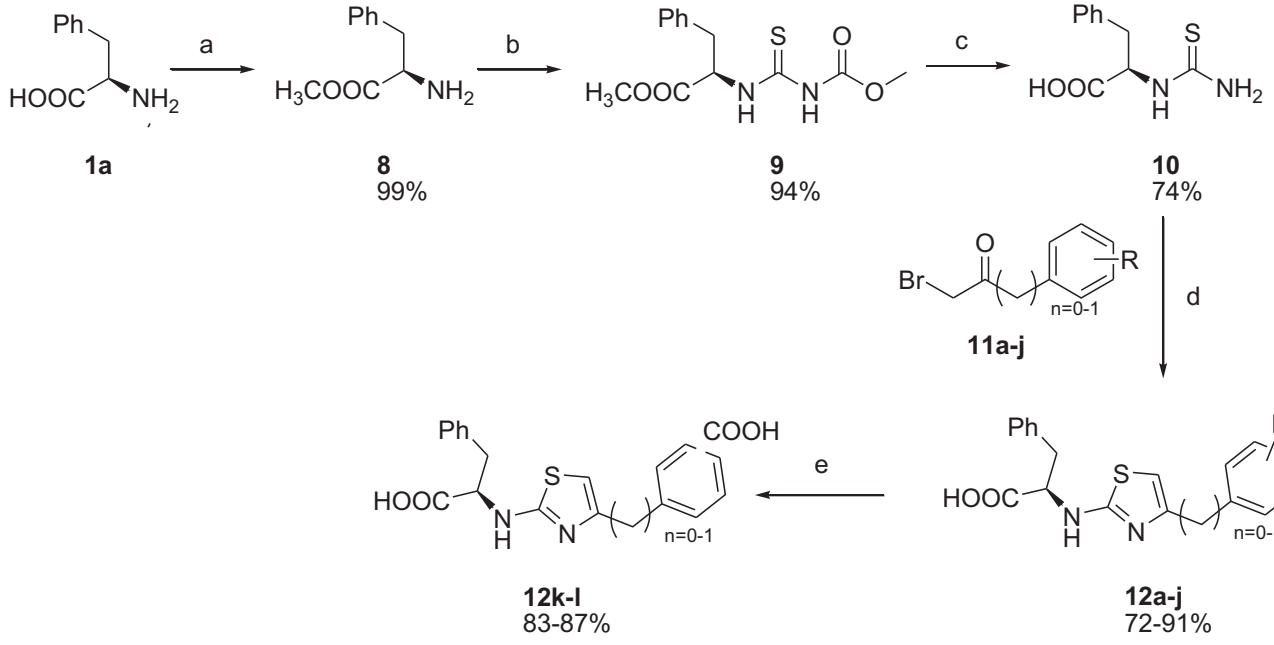

Scheme 3. [a]*Reagents and conditions*: (a) thionyl chloride, dry MeOH, 0 °C to r.t., 1 h; (b) methoxycarbonyl isothiocyanate, DIPEA, DCM, 0 °C to r.t., 1 h; (c) NaOH 3 N, MeOH, ref., 1 h; (d) DMF, r.t., 1–3 h; (e) NaOH/MeOH/THF, ref. 3 h. The substitution pattern of **11a–j** can be found in Table 2 within the description of the corresponding final products **12a–j**.

Please cite this article in press as: Mori M., et al. Bioorg. Med. Chem. Lett. (2018), https://doi.org/10.1016/j.bmcl.2018.01.031

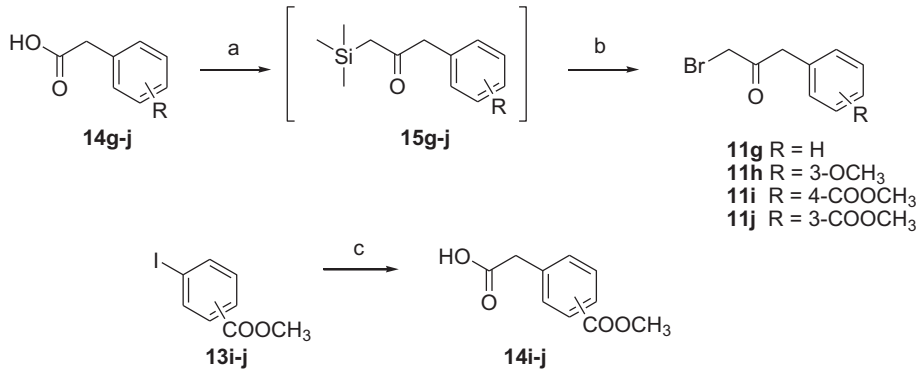

Scheme 4. [a]*Reagents and conditions*: (a) *i.* thionyl chloride, DMF, dry DCM, 0 °C to r.t., 30 min; *ii.* $TMSCH_2N_2$, dryCH_3CN, 0 °C to r.t., 1 h; (b) HBr 33%, dry CH_3CN, 0 °C to r.t., 2 h; (c) $PdCl_2$, AgOAc, NaOAc, AcOH, ref, 24 h.

Table 3
Inhibition of Mtb Zmp1 with rhodanines **5a**–**n** and **7a**–**b**, and aminothiazoles **12a**–**l**.

Cmpd	% Zmp1 residual activity at 50 μM	IC_{50} (μM)	Cmpd	% Zmp1 residual activity at 50 μM	IC_{50} (μM)
ZTB23(R)		0.87	**7a**	19.1	26.9
5a	13.4	9.3	**7b**	10.4	11.4
5b	13.2	12.5	**12a**	91.9	n.d.
5c	13.5	24.0	**12b**	35.0	41.3
5d	28.1	43.9	**12c**	100	n.d.
5e	58.7	n.d.	**12d**	36.3	35.7
5f	12.3	20.4	**12e**	100	n.d.
5g	10.0	18.4	**12f**	100	n.d.
5h	7.1	6.6	**12g**	100	n.d.
5i	7.2	2.9	**12h**	100	n.d.
5j	12.7	1.3	**12i**	61.0	n.d.
5k	12.6	23.4	**12j**	100	n.d.
5l	10.3	3.9	**12k**	100	n.d.
5m	11.2	15.7	**12l**	100	n.d.
5n	18.9	28.2			

n.d. = not determined – Zmp1 residual activity above the threshold.

gest Zmp1 inhibitor among rhodanines bearing D-phenylalanine. Finally, the replacement of the distal phenyl ring with the bioisosteres thiophene or pyridine does not provide significant benefits (see **7a**–**b**). In the Zn-binding portion of the inhibitors, D-phenylalanine provided generally stronger Zmp1 inhibition than D-alanine and glycine, even though an exception to this trend was observed for the D-alanine derivative **5j** that showed stronger inhibition of Zmp1 compared to the corresponding D-phenylalanine **5a**. Besides, rhodanines bearing bulky D-amino acids inhibit Zmp1 more potently than glycine, S-amino acids[18] and D-amino acids endowed with a small side chains.

Only aminothiazoles **12b** and **12d** inhibited Zmp1 with a potency above the threshold thus providing insufficient data for SAR analysis. However, the aminothiazole scaffold emerged as new possible chemotype of Zmp1 inhibitors that is worth of further investigation.

The possible binding mode of compounds to Zmp1 catalytic site[17] was investigated by molecular docking simulations (computational details in Supporting Information).[18] We describe here the binding mode of **5j** that was the most potent Zmp1 inhibitor studied in this work, **5h** that was the most potent among D-phenylalanine bearing rhodanines, and **12d** that was the most potent among aminothiazols (Fig. 2). Overall, the amino acid carboxylic group of **5j**, **5h** and **12d** coordinates the catalytic Zn(II) ion by a canonical geometry,[17,18,24] while H-bonding to key residues Glu494 and His622 (Fig. 2); the side chain is projected towards the solvent area. Different from the aminothiazole, the rhodanine core establishes an H-bond with Asn452 that may explain its stronger inhibitory potency. Moving to the distal groups, the *meta*-carboxylic function of **5j** is H-bonded to Arg628 and Thr606, while the phenyl ring is π-π stacked to Phe48 (Fig. 2A). The *para*-nitrile substituent of **5h** establishes an H-bond with Thr606 (Fig. 2B) although its steric hindrance does not allow the phenyl ring to π-π stack with Phe48, which may explain the slightly weaker potency of **5h** compared to **5j**. Finally, the nitro group of the aminothiazole **12d** is H-bonded to Thr606 (Fig. 2C) but also in this case no π-π stacking with Phe48 is observed. Docking poses correlate with SAR, thus providing hints for further structure-guided design and optimization studies.

Compounds **5a**, **5b** and **5c** showed a very low activity *in vitro* against isolated Mtb H37Ra ATCC 25177 (experimental procedures in Supporting Information), with MIC values of 64 mg/L or higher (Table 4). This is consistent with the fact that Zmp1 is secreted by Mtb, and its targeting should not impair directly Mtb replication outside the host cell. With the exception of **5a**, which showed CC_{50} values higher than 100 μg/ml both in Vero and THP-1 cell lines, **5b** and **5c** showed CC_{50} at concentrations much lower than the MICs. However, **5a** and **5c** exhibited a significant inhibition of the growth of Mtb in THP-1 infected cells also at a concentration as low as 10 μg/ml (23.4 and 53.8%, respectively, Table 4). Zmp1 inhibitors identified previously **ZTB23(S)** and **ZTB23(R)** showed inhibition of Mtb growth in THP-1 infected cells comparable to **5a** at 100 μg/ml (Table 4). Furthermore, 10 μg/ml of **5c** induced a 53.8% inhibition of Mtb growth, comparable with **ZTB23(S)** and much higher than **ZTB23(R)** at the same concentration.

Novel therapeutic agents able to eradicate latent Mtb from the host are highly desirable to complement the current anti-TB warheads. Here, with the aim to address SAR of the rhodanine scaffold

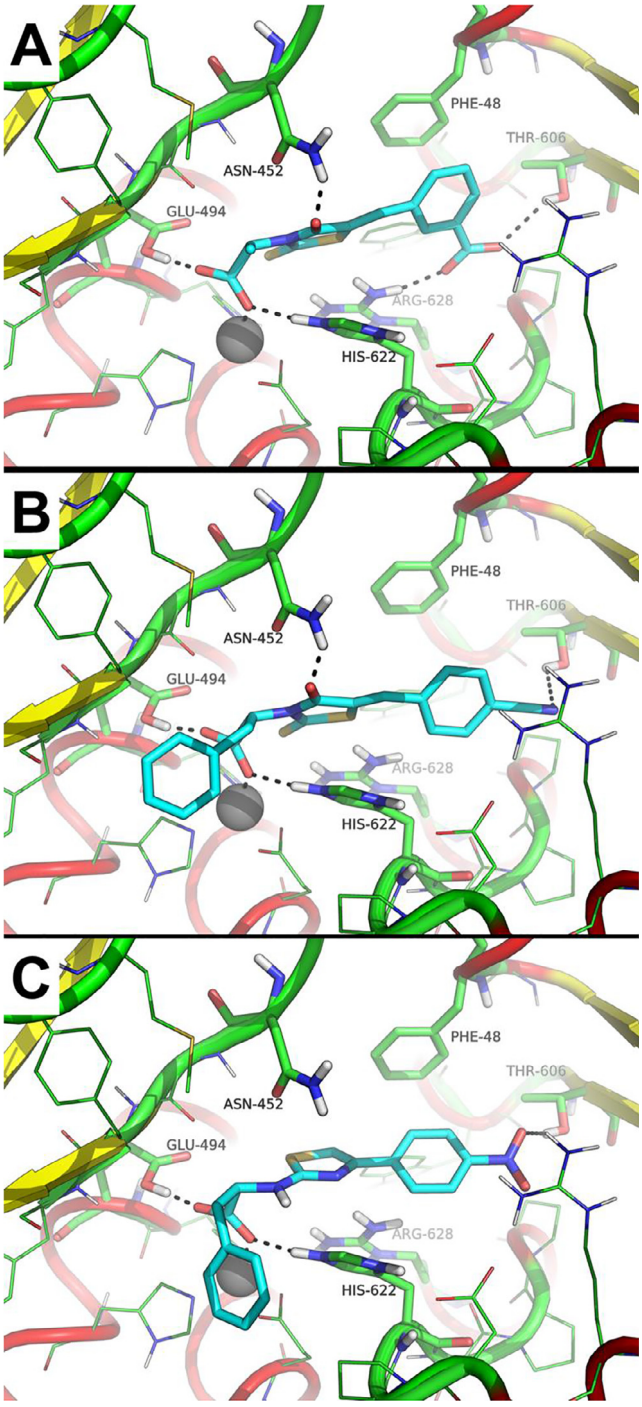

Fig. 2. Predicted binding mode of **5j** (A), **5h** (B), and **12d** (C) within the catalytic active site of Zmp1. The protein secondary structure is shown as colored cartoon (red = alpha helix; yellow = beta sheet; green = loop); residues within 5 Å from the ligands are shown as lines, while those interacting with the inhibitors are shown as sticks and are labeled. The catalytic Zn(II) ion is shown as a grey sphere, while main polar contacts between Zmp1 and small molecules are showed as black dashed lines.

identified in a prior work,[18] a number of rhodanines and aminothiazoles were designed, synthesized and tested against the recombinant Zmp1 enzyme from Mtb as well as in a cellular model system of TB infection. Rhodanine emerged as a privileged scaffold for

Table 4
MIC, cytotoxicity and macrophage assay of tested compounds.

Cmpd	CC_{50} Vero [μg/ml]	CC_{50} THP-1 [μg/ml]	MIC [μg/ml]	% inhibition of Mtb growth in THP-1	
				10 μg/ml	100 μg/ml
ZTB23(S)	>125	115.0	>64	57.4 ± 2.5	58.3 ± 2.9
ZTB23(R)	>125	>125	>64	0.1 ± 2.2	60.0 ± 2.6
5a	>125	101.9	>64	23.4 ± 2.9	54.5 ± 2.6
5b	32.5	21.9	64	0.5 ± 3.0	ND
5c	23.2	11.2	64	53.8 ± 3.4	ND

ND = Not Determined (tested concentration is above the CC_{50} value).

Zmp1 inhibition compared to the aminothiazole (this latter becoming – however – worth of investigation). In fact, almost all rhodanines (**5a–d**, **5f–n**, and **7a–b**) showed inhibition of recombinant Zmp1 with IC_{50} values in the range 1.3–43.9 μM, whereas only two aminothiazoles (namely, **12b** and **12d**) proved active with IC_{50} values of 41.3 and 35.7 μM, respectively. The druggability of the Zmp1 was further substantiated *in vitro* against THP-1 infected cells, where rhodanines **5a** and **5c** exhibited 23.4 and 53.8% of Mtb growth inhibition, respectively, at the non-toxic concentration of 10 μg/ml. For the first time we showed that rhodanine-derived Zmp1 inhibitors impair the growth of Mtb in infected macrophages at low concentrations, which opens new venues to further developing these molecules up to anti-TB lead candidates.

Declaration of interest

None.

A. Supplementary data

Supplementary data associated with this article can be found, in the online version, at https://doi.org/10.1016/j.bmcl.2018.01.031.

References

1. Global Tuberculosis Report 2015. WHO. ISBN 978 92 4 156505 9.
2. Kim JY, Mukherjee JS, Rich ML, Mate K, Bayona J, Becerra MC. *Tuberculosis (Edinburg)*. 2003;83:59.
3. Chaudhury RR, Thatte U. *Natl Med J India*. 2003;16:321.
4. Rowland K*Nature News*. <http://www.nature.com/news/totally-drug-resistant-tb-emerges-in-india-1.9797>.
5. Ioerger TR, O'Malley T, Liao R, et al. *PLoS One*. 2013;8:e75245.
6. Ehmann DE, Lahiri SD. *Curr Opin Pharmacol*. 2014;18:76.
7. Mdluli K, Ma Z. *Infect Disord Drug Targets*. 2007;7:159.
8. Koul A, Herget T, Klebl B, Ullrich A. *Nat Rev Microbiol*. 2004;2:189.
9. Mascarello A, Chiaradia-Delatorre LD, Mori M, Terenzi H, Botta B. *Curr Pharm Des*. 2016;22:1561.
10. Zhang CQ, Song XQ, Zhao Y, et al. *J Clin Lab Anal*. 2015;29:375.
11. Vemula MH, Medisetti R, Ganji R, et al. *Front Microbiol*. 2016;7.
12. Sander P, Clark S, Petrera A, et al. *Vaccine*. 2015;33:1353.
13. Petrera A, Amstutz B, Gioia M, et al. *Biol Chem*. 2012;393:631.
14. Vemula MH, Ganji R, Sivangala R, et al. *Front Microbiol*. 2016;7.
15. Master SS, Rampini SK, Davis AS, et al. *Cell Host Microbe*. 2008;3:224.
16. Muttucumaru DG, Smith DA, McMinn EJ, Reese V, Coler RN, Parish T. *Tuberculosis (Edinburg)*. 2011;91:111.
17. Ferraris DM, Sbardella D, Petrera A, et al. *J Biol Chem*. 2011;286:32475.
18. Mori M, Moraca F, Deodato D, et al. *Bioorg Med Chem Lett*. 2014;24:2508.
19. Subhedar DD, Shaikh MH, Nawale L, et al. *Bioorg Med Chem Lett*. 2016;26:2278.
20. Subhedar DD, Shaikh MH, Shingate BB, et al. N. *Eur J Med Chem*. 2017;125:385.
21. Lee CL, Sim MM. *Tetrahedron Lett*. 2000;41:5729.
22. Tomasic T, Masic LP*Privileged Scaffolds in Medicinal Chemistry: Design, Synthesis, Evaluation*. Cambridge: Royal Society of Chemistry; 2015:214.
23. *Hantzsch Thiazole Synthesis*. Wiley Online Library; 2010.
24. Mori M, Massaro A, Calderone V, Fragai M, Luchinat C, Mordini A. *ACS Med Chem Lett*. 2013;4:565.